JCI The Journal of Clinical Investigation

Basal cell carcinomas in mice arise from hair follicle stem cells and multiple epithelial progenitor populations

Marina Grachtchouk, … , Monique Verhaegen, Andrzej A. Dlugosz

J Clin Invest. 2011;121(5):1768-1781. https://doi.org/10.1172/JCI46307.

Research Article

Uncontrolled Hedgehog (Hh) signaling leads to the development of basal cell carcinoma (BCC), the most common human cancer, but the cell of origin for BCC is unclear. While Hh pathway dysregulation is common to essentially all BCCs, there exist multiple histological subtypes, including superficial and nodular variants, raising the possibility that morphologically distinct BCCs may arise from different cellular compartments in skin. Here we have shown that induction of a major mediator of Hh signaling, GLI2 activator (GLI2ΔN), selectively in stem cells of resting hair follicles in mice, induced nodular BCC development from a small subset of cells in the lower bulge and secondary hair germ compartments. Tumorigenesis was markedly accelerated when GLI2ΔN was induced in growing hair follicles. In contrast, induction of GLI2ΔN in epidermis led to the formation of superficial BCCs. Expression of GLI2ΔN at reduced levels in mice yielded lesions resembling basaloid follicular hamartomas, which have previously been linked to low-level Hh signaling in both mice and humans. Our data show that the cell of origin, tissue context (quiescent versus growing hair follicles), and level of oncogenic signaling can determine the phenotype of Hh/Gli-driven skin tumors, with high-level signaling required for development of superficial BCC-like tumors from interfollicular epidermis and nodular BCC-like tumors from hair follicle stem cells.

 Related Commentary, page 1681

Basal cell carcinomas in mice arise from hair follicle stem cells and multiple epithelial progenitor populations

Marina Grachtchouk,[1] Joanna Pero,[1] Steven H. Yang,[1,2] Alexandre N. Ermilov,[1] L. Evan Michael,[1,2] Aiqin Wang,[1] Dawn Wilbert,[1] Rajiv M. Patel,[1,3] Jennifer Ferris,[1] James Diener,[1] Mary Allen,[1] Seokchun Lim,[1] Li-Jyun Syu,[1] Monique Verhaegen,[1] and Andrzej A. Dlugosz[1,2,4]

[1]Department of Dermatology, [2]Cellular and Molecular Biology Program, [3]Department of Pathology, and [4]Department of Cell and Developmental Biology, University of Michigan Medical School, Ann Arbor, Michigan, USA.

Uncontrolled Hedgehog (Hh) signaling leads to the development of basal cell carcinoma (BCC), the most common human cancer, but the cell of origin for BCC is unclear. While Hh pathway dysregulation is common to essentially all BCCs, there exist multiple histological subtypes, including superficial and nodular variants, raising the possibility that morphologically distinct BCCs may arise from different cellular compartments in skin. Here we have shown that induction of a major mediator of Hh signaling, GLI2 activator (GLI2ΔN), selectively in stem cells of resting hair follicles in mice, induced nodular BCC development from a small subset of cells in the lower bulge and secondary hair germ compartments. Tumorigenesis was markedly accelerated when GLI2ΔN was induced in growing hair follicles. In contrast, induction of GLI2ΔN in epidermis led to the formation of superficial BCCs. Expression of GLI2ΔN at reduced levels in mice yielded lesions resembling basaloid follicular hamartomas, which have previously been linked to low-level Hh signaling in both mice and humans. Our data show that the cell of origin, tissue context (quiescent versus growing hair follicles), and level of oncogenic signaling can determine the phenotype of Hh/Gli-driven skin tumors, with high-level signaling required for development of superficial BCC-like tumors from interfollicular epidermis and nodular BCC-like tumors from hair follicle stem cells.

Introduction

Identifying the cells of origin of human neoplasms remains a major challenge in cancer biology (1). Skin is a useful organ for exploring this issue experimentally because it is highly accessible and contains well-defined stem cell and transit-amplifying cell compartments and because robust approaches have been developed for the generation of mouse models of epithelial skin cancer that faithfully recapitulate many of the features seen in human skin cancer (reviewed in refs. 2, 3). Moreover, the influence of tissue regeneration on tumorigenesis can be easily studied during epidermal wound healing or during different phases of the hair growth cycle. This is a repetitive, physiological process that comprises periods of epithelial proliferation, differentiation, and hair elongation (anagen); apoptosis-driven hair follicle regression (catagen), which spares the follicle stem cell compartments; and a resting phase (telogen), during which hair follicle stem cells are largely quiescent (4). Programmed activation of epithelial stem cells takes place at the onset of each anagen phase, followed by brisk proliferative expansion of hair follicle progenitor cells (5), providing a unique opportunity to compare the responsiveness to oncogenic stimuli of quiescent stem cells versus their transit-amplifying progeny.

Non-melanoma skin cancers are the most common neoplasms in humans, and the great majority of these tumors are basal cell carcinomas (BCCs) (6). Nearly all BCCs exhibit uncontrolled activation of the Hedgehog (Hh) signaling pathway, one of a handful of critical pathways that orchestrate embryonic patterning and development and can contribute to tumor formation when deregulated after birth (7). Whereas physiologic Hh signaling is spatially restricted, generally intermittent, and dependent on the presence of secreted Hh ligands (8), oncogenic Hh signaling in BCC is continuous and Hh ligand–independent (6). Mutation-driven, deregulated Hh signaling in BCC occurs most frequently due to loss of the Hh receptor/signaling repressor PTCH1 or mutational activation of the signaling effector smoothened (SMO) (reviewed in ref. 9). Regardless of the initiating oncogenic event, expression of target genes regulated by Hh-responsive Gli transcription factors is highly elevated in essentially all BCCs. Moreover, findings in several mouse models strongly support the idea that uncontrolled Hh/Gli signaling plays a pivotal role in, and may be sufficient for, the development of BCC and related skin tumors (reviewed in refs. 9, 10).

Studies examining the normal functions of Hh signaling in different organs have provided clues as to where, and how, deregulated Hh signaling contributes to the development of cancer (7). In skin, physiologic Hh signaling is activated in growing hair follicles, where it is required for proliferation of hair follicle epithelium during morphogenesis (11–13). Hh responses in mice are mediated by Gli2, the primary transcriptional effector of Hh signaling (14, 15), which regulates follicle proliferation by inducing cyclins D1 and D2 (15). The Hh pathway is also required for postnatal growth of hair follicles (16). Since Hh signaling is a major regulator of physiologic hair growth via stimulation of proliferation of epithelial hair follicle progenitors, it has been argued that these cells possess intracellular signaling machinery rendering them preferentially susceptible to Hh pathway–driven tumorigenesis as well. This concept is in keeping with studies underscoring the morphological and biochemical similarities between human hair follicles and

Conflict of interest: The authors have declared that no conflict of interest exists.
Citation for this article: *J Clin Invest.* 2011;121(5):1768–1781. doi:10.1172/JCI46307.

BCCs (17–19), which have led to the proposal that BCCs are follicle-derived tumors (reviewed in refs. 20, 21).

Although the molecular hallmark of nearly all BCCs is elevated Hh signaling, which is the oncogenic driver for these tumors, there is considerable morphological heterogeneity among BCCs, with nodular and superficial subtypes being among the most common (22, 23). Superficial BCCs are thin, pink lesions ranging in size from a few millimeters to several centimeters in diameter and are characterized histologically by downgrowths of basaloid-appearing cells that appear to arise directly from interfollicular epidermis. Nodular BCCs are generally more substantive and may appear as a pink or red papule in the skin, with masses of basaloid cells situated within the dermis and occasionally extending into the subcutaneous fat. In contrast to superficial BCC, histological sections of nodular BCC frequently show no connection to the overlying epidermis, raising the possibility that this BCC subtype may arise from epithelial cells in hair follicles that extend deep into the dermis.

A recent study investigated the cell of origin of mouse BCC using an oncogenic form of Smo that was induced in hair follicles and interfollicular epidermis in Cre-inducible mouse models (24). The investigators concluded that murine BCCs derive almost exclusively from the epidermis, with a small minority of tumors arising from hair follicle infundibulum. Intriguingly, targeting of Smo directly to hair follicle stem cells did not produce tumors, suggesting that the stem cell niche is refractory to Hh pathway–driven transformation. These results were unanticipated, since data from several other mouse models point to the hair follicle as the site of origin for BCC (25–34). However, none of these earlier studies directly targeted the stem cell compartment, making it impossible to formally exclude the possibility that tumor initiation occurs in another compartment(s) but proliferative expansion into a detectable tumor can only take place when cells have migrated into the hair follicle. Moreover, we have previously shown that expression of oncogenic SMO in skin leads to benign tumors resembling basaloid follicular hamartomas rather than BCCs, which appear to require a higher level of Hh signaling for their development (25, 35, 36).

Here, we tested whether hair follicle stem cells or their progeny can give rise to Hh-activated nodular skin tumors using a novel mouse model that combines Cre-*lox* and tet-regulated systems to achieve tight control of GLI2 activator (GLI2ΔN) expression in epithelial compartments of the hair follicle. We show that nodular BCC-like tumors arise from hair follicle stem cells or their transient-amplifying progeny, while superficial BCC-like tumors arise from the interfollicular epidermis. Expression of low levels of GLI2ΔN in skin leads to the development of benign tumors resembling basaloid follicular hamartomas previously described in mice expressing an activated *SMO* allele (35, 36), rather than nodular BCC-like tumors. Our data support the concept that both the cell of origin and the level of oncogenic signaling influence the phenotype of Hh/Gli-activated skin tumors, with follicle stem cell–derived, nodular BCC-like tumors requiring high-level Hh pathway activity.

Results

Conditional GLI2ΔN expression in hair follicle stem cells and their progeny. We generated a conditional, triple-transgenic model that combines Cre-*lox* and tet-regulated gene-switch technologies to achieve tight control of transgene expression, both spatially and temporally, in hair follicle stem cells or a wide variety of other cell populations. The 3 components of this model include a transgenic Cre driver; a *ROSA26* promoter–based, Cre-inducible (lox-STOP-lox) reverse tet transcriptional activator (rtTA) strain (37), which we designate *R26-LSL-rtTA*; and a *tetO*-regulated effector strain, in which transgene expression can be induced by doxycycline when rtTA transactivator is present (Figure 1A). Targeting specificity is governed by the choice of Cre driver, while the oncogenic stimulus is provided by the specific *tetO* effector mouse, making this a versatile model for manipulating essentially any oncogenic pathway in any organ, if appropriate Cre and *tetO* lines are available. Importantly, because rtTA induction is Cre dependent and under the control of the ubiquitously expressed *ROSA26* promoter, rtTA will be expressed in all cells that have undergone a Cre-mediated recombination event, as well as their progeny. In addition, by altering the doxycycline treatment regimen, transgene expression can be induced to different levels. For the experiments in this study, we generated *tetO-GLI2ΔN* mice, since we had previously shown that GLI2ΔN and the analogous mouse allele, Gli2ΔN2, are potent activators of oncogenic Hh signaling and drive BCC-like skin tumor development in mice (38, 39).

Nodular BCC-like skin tumors arise from resting hair follicle stem cells. To test whether hair follicle stem cells are competent to form skin tumors in response to GLI2ΔN, we used *K15-CrePR1* mice, which have previously been shown to have Cre recombinase activity in stem cells in the bulge and secondary hair germ of the telogen follicle following treatment with the progesterone analog RU486 (ref. 40, Figure 1, B and C, and Supplemental Figure 1; supplemental material available online with this article; doi:10.1172/JCI46307DS1). We generated *K15-CrePR1;R26-LSL-rtTA;tetO-GLI2ΔN* (*iK15;rtTA;GLI2ΔN*) triple-transgenic mice, which we treated with RU486 to activate Cre function, and induced rtTA following Cre-mediated excision of the elements inhibiting its expression. We then treated mice with doxycycline starting at 7 weeks of age to induce GLI2ΔN expression. Because the first few hair cycles in dorsal mouse skin are synchronized, essentially all hair follicles in this region are in a prolonged telogen (resting) phase of the hair cycle at this time (ref. 41 and Figure 1D), so any effects of GLI2ΔN on cell proliferation will not be obscured by physiologic hair follicle growth in anagen.

Although dorsal skin appeared grossly normal after 3 weeks of doxycycline treatment, multiple microscopic skin tumors were detected at this time. Tumor nodules were located within the dermis and comprised masses of basaloid-appearing cells with scant cytoplasm resembling human BCC (Figure 1E). The histology of early-stage tumors suggested that they are derived from the secondary hair germ, with more proximal regions of the bulge largely unaffected (Figure 1, B and E). In keeping with the expression pattern of the promoter in *K15-CrePR1* mice (40), the sebaceous glands, upper hair follicle, and epidermis were largely unaffected (Figure 1E). Hair follicle–associated tumors were observed at multiple other sites, including the tail, ear, dorsal paw, and snout (Figure 1F). Tumors on the snout and dorsal paws developed more rapidly than at other sites, with grossly visible tumors seen at 3 weeks of treatment when only microscopic tumors were evident elsewhere. Large tumors sometimes contained regions of central necrosis (not shown), as occasionally seen in human BCCs.

In addition to a nodular BCC-like morphology, immunophenotyping revealed a pattern of lineage markers characteristic of human BCC. Tumors expressed keratins K5 and K17 and Sox9 (42); exhibited undetectable or negligible levels of keratins K1 and K6; and were hyperproliferative, based on Ki67 immunostaining (Figure 2A). Immunostaining for MYC revealed expression of epitope-tagged GLI2ΔN in tumor cells, with relatively few MYC-positive cells

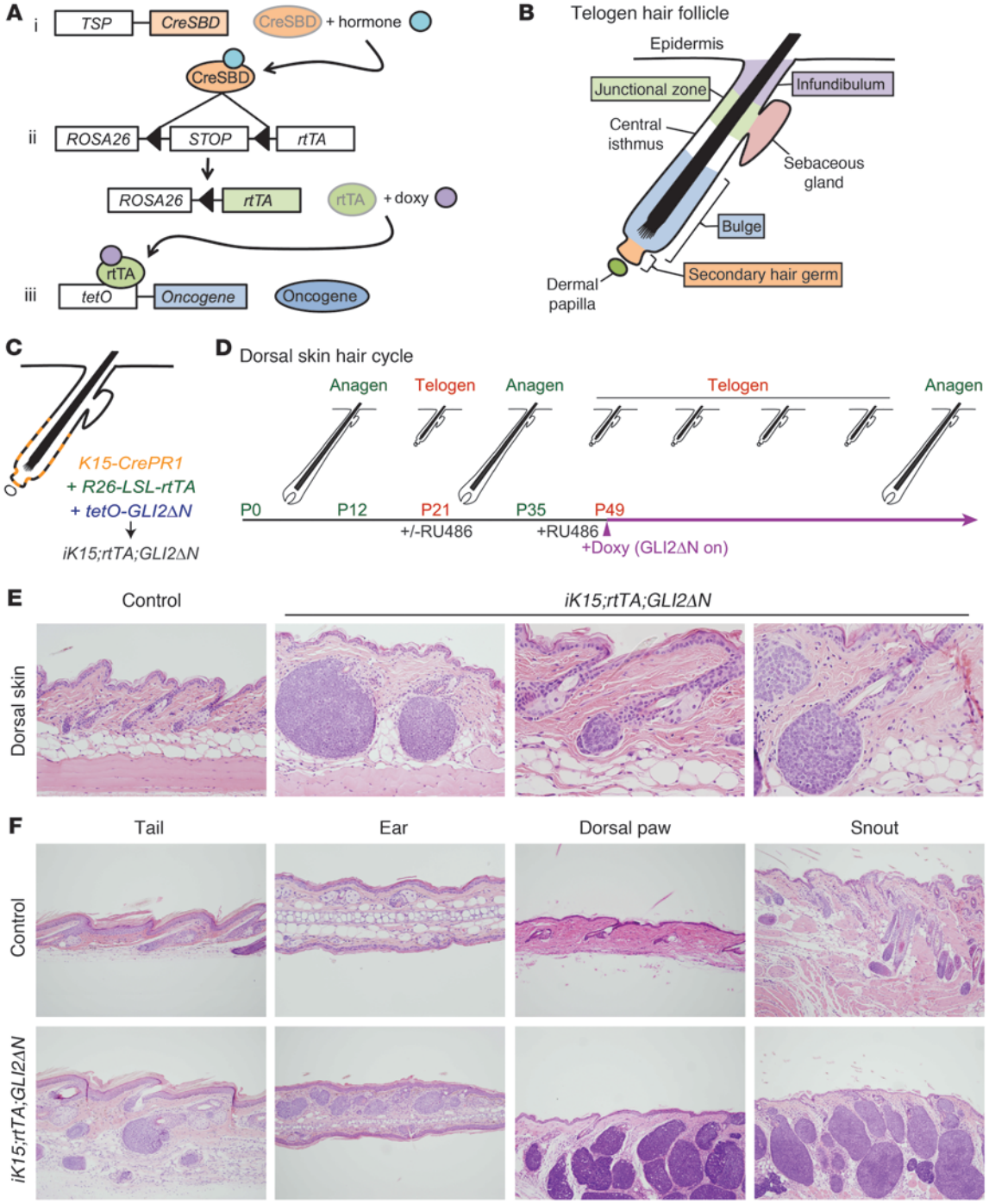

Figure 1

BCC-like skin tumors arise from hair follicle stem cells. (**A**) General scheme showing triple-transgenic model combining Cre-*lox* and tet/doxycycline-regulated technologies to achieve tight spatial and temporal control of transgene expression. The 3 components include mouse strains carrying: (i) a tissue-specific promoter (TSP) driving expression of a hormone-inducible Cre allele fused to a steroid binding domain (CreSBD); (ii) a Cre-inducible "tet on" rtTA, under the control of the ubiquitously expressed *ROSA26* promoter (*R26-LSL-rtTA*) (37); and (iii) an oncogene downstream of multiple *tetO* sequences and minimal CMV promoter that is induced by rtTA when doxycycline (doxy) is present. (**B**) Cellular compartments in a quiescent (telogen) hair follicle. Most hair follicle stem cells are localized to the bulge and secondary hair germ compartments. (**C**) Compartments in which *K15-CrePR1* mice can drive recombination in *K15-CrePR1;R26-LSL-rtTA;tetO-GLI2ΔN* (*iK15;rtTA;GLI2ΔN*) mice to activate rtTA expression. (**D**) Synchronized hair growth cycle in postnatal mouse skin, with approximate mouse ages and timing of doxycycline treatment/GLI2ΔN transgene induction indicated. (**E**) Spontaneous development of microscopic skin tumors from telogen hair follicle stem cells in dorsal skin of *iK15;rtTA;GLI2ΔN* mice, after 3 weeks of doxycycline treatment. Note tumor development from lowermost follicle in a region corresponding to the secondary hair germ. Original magnification, ×200 (left panel); ×400 (right panels). (**F**) Spontaneous tumor development from $K15^+$ follicle stem cells at other body sites 3 weeks after GLI2ΔN induction. Original magnification, ×100 (tail, dorsal paw, and snout); ×200 (ear).

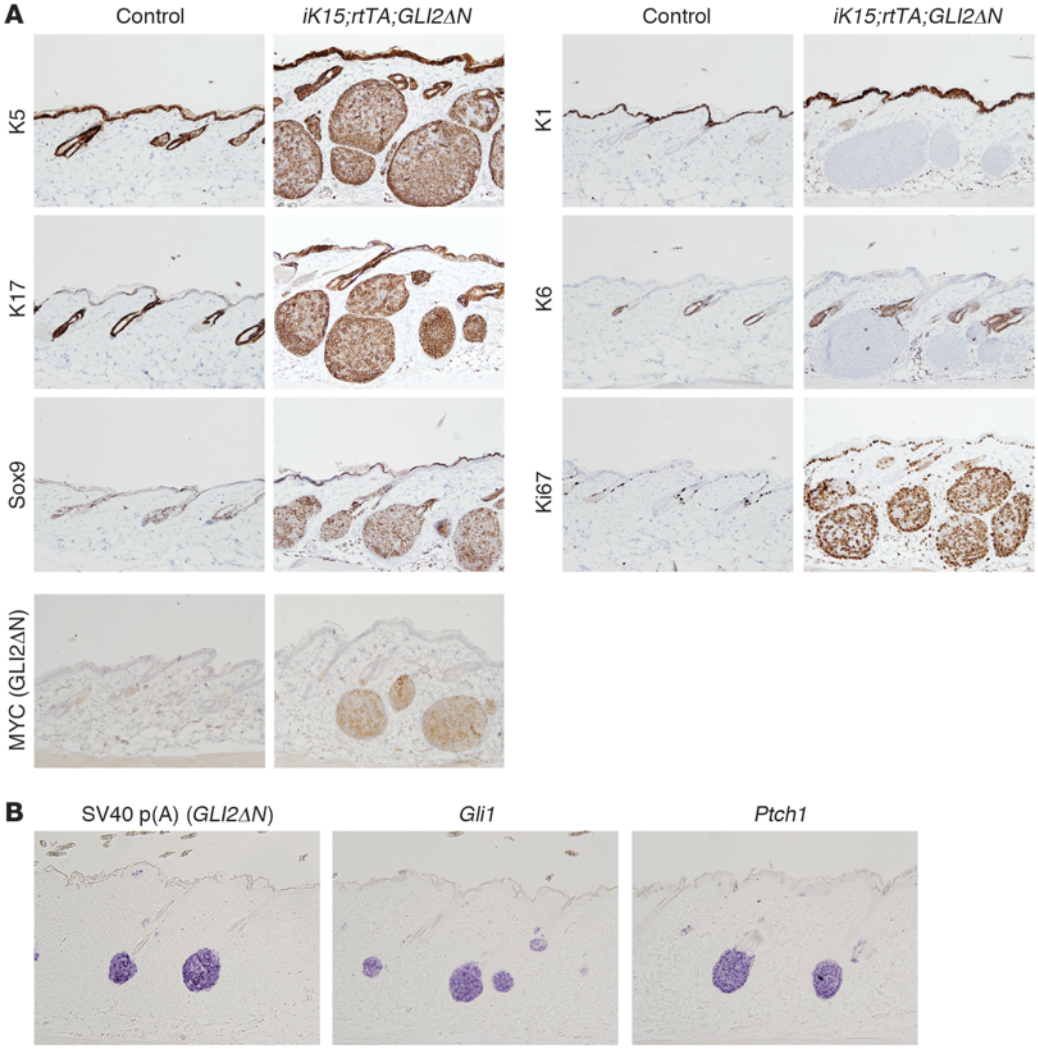

Figure 2
Nodular skin tumors arising from K15+ stem cells express BCC markers. (**A**) Immunostaining showing BCC-like keratin profile (K5 and K17 expressed, K1 and K6 not expressed). Tumor cells also express the BCC marker Sox9 and are highly proliferative, based on Ki67 immunostaining. BCC-like tumors also express MYC-tagged GLI2ΔN transgene product. Original magnification, ×200. (**B**) In situ hybridization showing transcripts for Hh target genes *Gli1* and *Ptch1* in early-stage microscopic tumors, along with *GLI2ΔN*, detected using transgene-specific riboprobe against the SV40 poly(A) tail. Original magnification, ×200.

in normal-appearing hair follicles (Figure 2A), suggesting that the recombination efficiency using our protocol was relatively low. This was corroborated using RU486-treated *K15-CrePR1;R26R* mice carrying a Cre-inducible *lacZ* reporter allele (data not shown). In situ hybridization of early tumors revealed expression of GLI2ΔN transgene and Hh target genes *Gli1* and *Ptch1* (Figure 2B), which serve as molecular markers of deregulated Hh signaling in human BCC (9, 10). These results establish that *K15*-expressing stem cells in resting hair follicles of dorsal skin are competent to form nodular BCC-like skin tumors, which appear to arise preferentially from the secondary hair germ or lowermost bulge stem cell compartments.

Nodular BCC-like skin tumors arise from the Lrg5-expressing subset of follicle stem cells. Although the location of early-stage tumors in *iK15;rtTA;GLI2ΔN* mice (Figure 1E) suggests that they are derived from cells in the secondary hair germ or lowermost bulge, given the expression pattern of K15-driven recombination (Figure 1C) we cannot rule out the possibility that tumor initiation occurs in a cell within the bulge compartment but proliferative expansion requires migration into the neighboring secondary hair germ. To define more precisely which stem cell population in the telogen follicle can give rise to GLI2ΔN-driven BCC-like skin tumors, we used *Lgr5-CreER* mice, which drive recombination in a more limited distribution comprising the secondary hair germ and a subset of cells in the lowermost portion of the bulge (ref. 43, Figure 3A, and Supplemental Figure 1), to generate *Lgr5-CreER;R26-LSL-rtTA;tetO-GLI2ΔN* (*iLgr5;rtTA;GLI2ΔN*) mice. Mice were treated with tamoxifen to activate Cre function, and doxycycline was again started at week 7 to activate GLI2ΔN expression at a time when hair follicles in dorsal skin are in telogen (Figure 3B).

Similar to *iK15;rtTA;GLI2ΔN* mice, in which both the bulge and secondary hair germ compartment are targeted, *iLgr5;rtTA;GLI2ΔN* mice developed tumors on dorsal skin (Figure 3C) as well as tail,

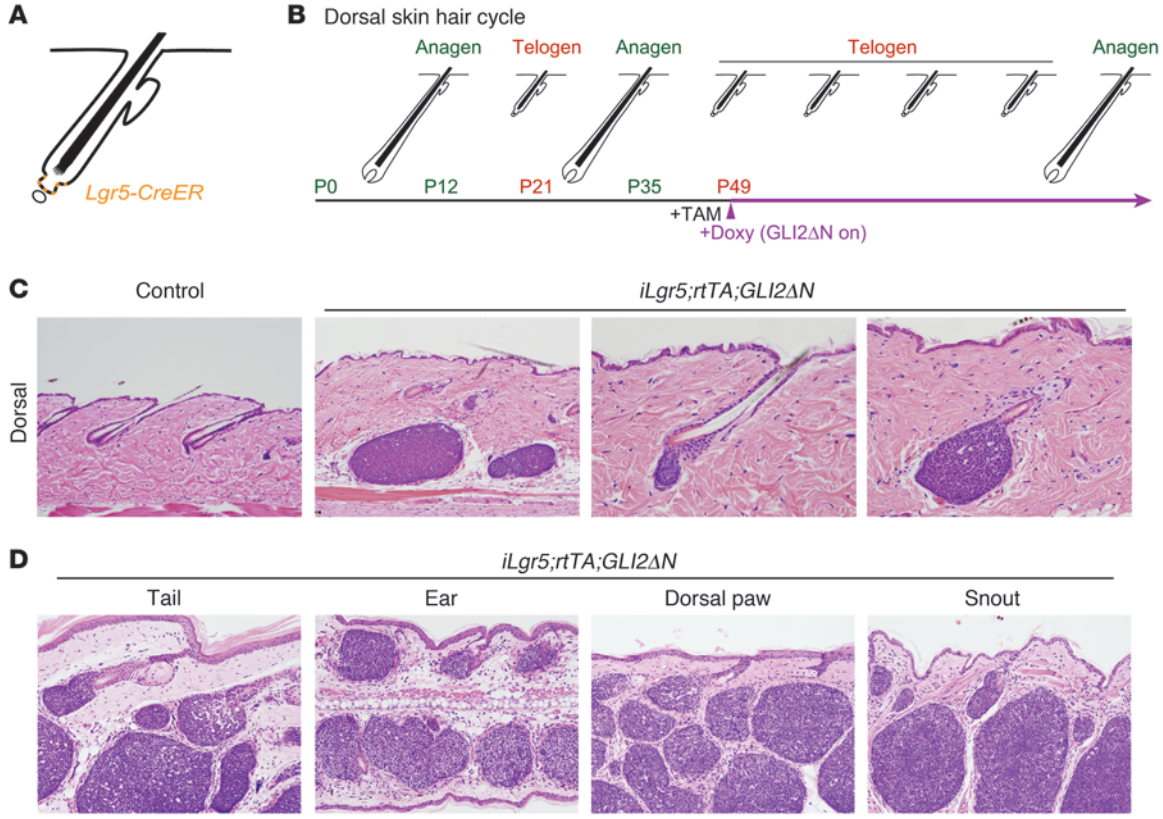

Figure 3
Robust BCC-like skin tumor development from the Lgr5⁺ subset of follicle stem cells. (**A**) *Lgr5-CreER*–driven recombination is limited to the secondary hair germ and lowermost bulge region. (**B**) Hair growth cycle and timing of doxycycline treatment/GLI2ΔN expression. TAM, tamoxifen. (**C**) Spontaneous development of microscopic skin tumors from telogen hair follicle stem cells in dorsal skin of *iLgr5;rtTA;GLI2ΔN* mice after 3 weeks of doxycycline treatment. Note early tumor development from the secondary hair germ. Original magnification, ×200 (left panels); ×400 (right panels). (**D**) Spontaneous nodular BCC-like tumor development from Lgr5⁺ follicle stem cells at other body sites. Original magnification, ×200.

ear, dorsal paw, and snout (Figure 3D). The kinetics of tumor induction in different body sites was similar to that of tumors arising in K15-targeted mice, with tumors appearing first on the snout and dorsal paws. The morphology of tumors was also similar to that arising in K15-targeted mice, and analysis of early-stage tumors revealed their derivation from the secondary hair germ or lowermost bulge region, with other compartments of the hair follicle and epidermis unaffected (Figure 3, C and D). These results identify the Lgr5⁺ subset of follicle stem cells as a source of progenitors for GLI2ΔN-driven BCC-like skin tumors and suggest that stem cells in the secondary hair germ and lowermost bulge are preferentially susceptible to Hh pathway–driven tumorigenesis.

Stem cells in the follicle bulge are resistant to GLI2ΔN-induced hyperplasia. The nearly exclusive development of GLI2ΔN-expressing tumors from cells in secondary hair germs of *iK15;rtTA;GLI2ΔN* mice (Figure 1E), despite K15-driven targeting to stem cells in the bulge as well, suggested that bulge cells may be resistant to transformation by GLI2ΔN. To explore this possibility and to assess the responsiveness of other epithelial cell populations in skin, we targeted GLI2ΔN expression broadly to the entire basal layer compartment throughout the resting hair follicle, sebaceous gland, and epidermis using *K14-rtTA;tetO-GLI2ΔN* (*K14;GLI2ΔN*) bitransgenic mice. Doxycycline treatment was started at 7 weeks, and mice were euthanized and tissue was collected for analysis after 2 and 5 days of GLI2ΔN transgene induction. By day 5, there was prominent expansion of proliferating basaloid cells in nearly all epithelial compartments of skin, including the epidermis, hair follicle infundibulum, sebaceous gland progenitors, and secondary hair germ (Figure 4A). In striking contrast, basaloid hyperplasia was not apparent in hair follicle epithelium between the hair germ and sebaceous gland, which includes the bulge compartment and adjacent central isthmus (Figure 1B and Figure 4A).

GLI2ΔN was detected by MYC immunostaining in hyperplastic basaloid cells of the epidermis, sebaceous gland, hair follicle infundibulum, and secondary hair germ, and at each of these sites there was a striking increase in proliferative activity detected by proliferating cell nuclear antigen (PCNA) immunostaining, which increased between 2 and 5 days of treatment (Figure 4B). Cells in the bulge region also expressed GLI2ΔN (Figure 4, B and E), but the fraction of these cells that was PCNA- or Ki67-positive was lower than that of GLI2ΔN-expressing epithelial cells in other regions (Figure 4, B and D). Coimmunostaining for PCNA and the bulge cell marker K15 confirmed that cells induced to proliferate in GLI2ΔN-expressing mice were normally quiescent bulge keratinocytes, both in tail and dorsal skin (Figure 4C). Thus, although basaloid hyperplasia suggestive of neoplastic transformation was not observed in the bulge during the time frame of this experiment, at least some cells in this stem cell compartment activated

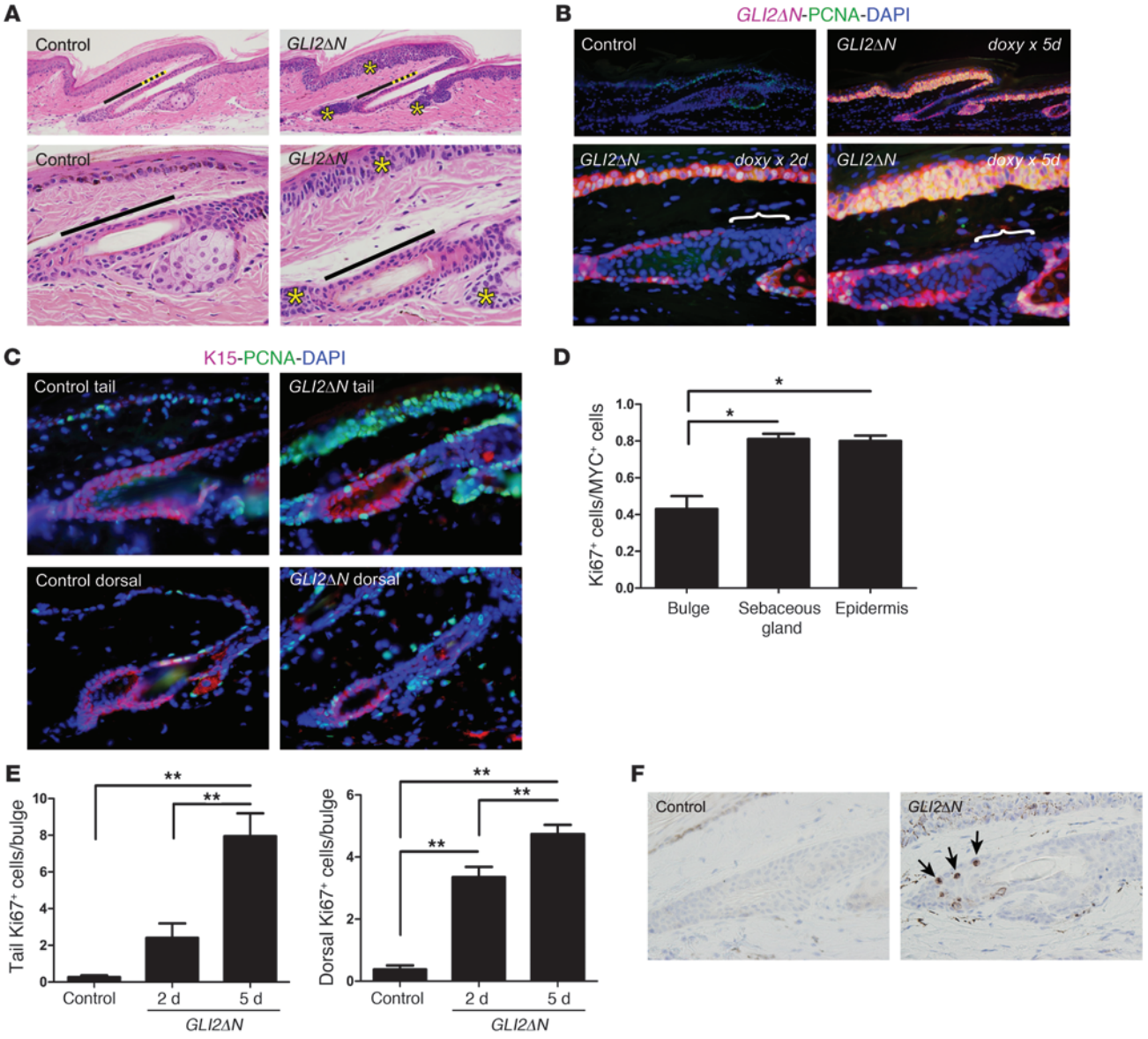

Figure 4

Impaired responsiveness of follicle bulge stem cells to acute induction of GLI2ΔN. (**A**) Histology of epithelial compartments in tail skin of control and *K14-rtTA;tetO-GLI2ΔN* (*K14;GLI2ΔN*) bitransgenic mice reveals basaloid cell hyperplasia in epidermis, sebaceous gland, and secondary hair germ (yellow asterisks in right panels), but not in the bulge or central isthmus (marked with black and dotted yellow bars, respectively). Original magnification, ×200 (upper panels); ×600 (lower panels). (**B**) Immunostaining for MYC reveals GLI2ΔN transgene expression in basal epithelial compartments, with the exception of cells in the central isthmus (white brackets). Coimmunostaining for GLI2ΔN (MYC) and PCNA reveals increased proliferation in all compartments expressing GLI2ΔN, although the fraction of PCNA$^+$ cells is lower in the bulge than other compartments (**D**). Original magnification, ×200 (upper panels); ×600 (lower panels). (**C**) Coimmunostaining for the bulge marker K15 and PCNA confirms proliferation in bulge stem cells in tail as well as dorsal skin. Original magnification, ×400. (**D**) Proliferative response to GLI2ΔN is approximately 50% lower in bulge cells than in epidermal or sebaceous gland cells. (**E**) Progressive increase in number of Ki67$^+$ normally quiescent bulge cells 2 and 5 days after activation of GLI2ΔN transgene expression by using doxycycline. Data in **D** and **E** are presented as mean ± SEM; $^*P < 0.05$, $^{**}P < 0.005$. (**F**) Increased apoptosis in bulge compartment of GLI2ΔN-expressing mice compared with controls, based on immunostaining for activated caspase-3 (arrows). Original magnification, ×600.

expression of proliferation markers in response to GLI2ΔN. Given the lack of basaloid hyperplasia in bulge cells (Figure 4A) and the absence of bulge-derived microscopic tumors (Figure 1E), we performed immunostaining to test whether GLI2ΔN expression leads to apoptosis. In contrast to controls, bulge compartments of *K14;GLI2ΔN* mice treated with doxycycline for 5 days contained cells expressing activated caspase-3 (Figure 4F). Thus, the selective resistance of bulge cells to GLI2ΔN-induced hyperplasia and tumorigenesis may be due to elimination via apoptosis of aberrantly proliferating cells in this stem cell compartment.

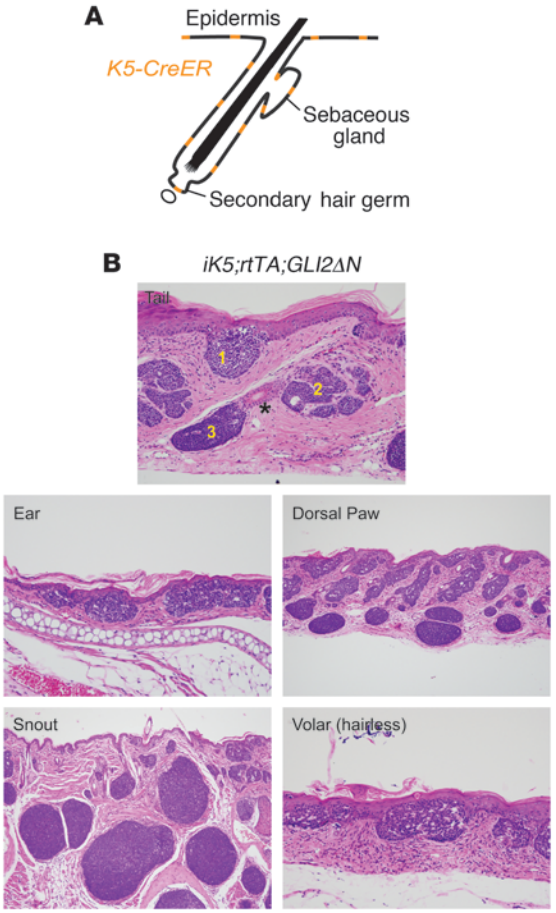

Figure 5
Induction of GLI2ΔN expression leads to BCC-like tumors derived from all 3 epithelial skin lineages. (**A**) Widespread potential recombination pattern for *K5-CreER* transgenic driver used to generate *iK5;rtTA;GLI2ΔN* mice. (**B**) Treatment with low-dose tamoxifen to drive recombination in a limited number of cells yielded BCC-like tumors in tail arising from epidermis (1), sebaceous gland (2), and lower follicle (3), with the bulge compartment (asterisk) unaffected. Superficial BCC-like tumor development in hairless skin confirms that these tumors can arise from interfollicular epidermis. Original magnification, ×200 (tail and ear); ×100 (dorsal paw and snout); ×400 (volar).

In addition to bulge cells, the central isthmus (Figure 1B), which contains the recently described Lgr6$^+$ stem cell compartment (44), was also relatively unaltered in *K14;GLI2ΔN* mice (Figure 4A). Remarkably, despite the predicted expression pattern of the *K14* promoter, which is expected to target all basal layer compartments (Supplemental Figure 1), basal cells in the central isthmus frequently had strikingly reduced or undetectable levels of GLI2ΔN relative to other basal layer populations (Figure 4B, brackets). Similar results were seen in *K5-rtTA;tetO-GLI2ΔN* mice (data not shown), in which transgene expression is also targeted to basal cell compartments in skin. While these results are in keeping with the idea that Hh signaling is tightly regulated in different stem cell compartments of the resting follicle via modulation of Gli protein levels (45–47), they may also reflect a reduction in or loss of *K14* and *K5* promoter activity in this region of the resting hair follicle. Collectively, the results of short-term GLI2ΔN induction studies indicate that, with the notable exception of cells residing within the bulge and possibly the central isthmus, multiple epithelial progenitor or stem cell populations in skin can give rise to basaloid hyperplasia following induction of GLI2ΔN expression, and that cells in each of these compartments may be competent to form BCC-like skin tumors.

BCC-like skin tumors can arise from hair follicle, sebaceous gland, and epidermal lineages. Because the severe phenotype of *K14;GLI2ΔN* mice precluded analysis beyond 10 days of transgene induction, to identify cell populations in skin that are competent to form BCC-like tumors, we again used the triple-transgenic model (Figure 1A), but with a conditional *K5-CreER* driver that can be activated in basal cell compartments in skin (Figure 5A, Supplemental Figure 1, and ref. 48). Low-dose tamoxifen was administered to *K5-CreER;R26-LSL-rtTA;tetO-GLI2ΔN* (*iK5;rtTA;GLI2ΔN*) mice to drive recombination in a limited number of K5-expressing cells, and GLI2ΔN expression was induced with doxycycline. Using this approach, we first noted skin abnormalities after 14 days, and by 21 days of treatment, histology revealed BCC-like tumors in skin from multiple body sites, including the tail, snout, dorsal paws, ears, and hairless volar skin (Figure 5B). As predicted based on cell populations responding to short-term GLI2ΔN induction (Figure 4), tumors appeared to arise from secondary hair germs, sebaceous glands, and epidermis, with epidermis-associated tumors (Figure 5B) resembling human superficial BCC. Taken together, these data reveal that oncogenic Hh signaling can drive BCC-like skin tumor development from several different epithelial progenitor populations in skin, although the BCC subtype (superficial versus nodular) is defined by the cell of origin (epidermis versus hair follicle, respectively).

Accelerated BCC-like tumor development from anagen hair follicles. Follicles during the second, prolonged telogen phase can be induced into a synchronized and premature anagen phase by either chemical (Nair) or physical (hair plucking) depilation, providing a convenient method for triggering synchronized hair follicle growth with precise timing (Figure 6A). Previous studies suggested that anagen hair follicles are particularly susceptible to Hh pathway–driven tumorigenesis (29, 32), raising the possibility that activated follicle stem cells or transit-amplifying progeny are tumor progenitors in this setting. To examine this possibility, we induced GLI2ΔN expression in *iK15;rtTA;GLI2ΔN* or *iLgr5;rtTA;GLI2ΔN* transgenic mice in early anagen, rather than telogen (Figure 6A). Dorsal hair was clipped during the second telogen phase of the hair cycle; unscheduled anagen was induced using either Nair or hair plucking; and 1 day later, GLI2ΔN transgene was induced by administration of doxycycline. As expected, induction of anagen in control mice led to hair follicle elongation and grossly apparent hair growth, whereas anagen-induced regions of skin in *iK15;rtTA;GLI2ΔN* mice contained grossly evident tumors by 14–15 days of transgene expression (Figure 6, B and C). Telogen follicles in surrounding skin were largely unaffected (Figure 6C), with the exception of occasional microscopic tumors as described above (Figure 1E). Similar results were seen using *iLgr5;rtTA;GLI2ΔN* mice (data not shown). The differential response of telogen versus anagen follicles was highly consistent: telogen dorsal skin of all *iK15;rtTA;GLI2ΔN* mice examined (n = 7) appeared grossly normal after 2 weeks of GLI2ΔN induction, while 100% of mice (n = 18) with anagen-induced dorsal skin had gross evidence of tumor development at the same time point. The accelerated development of BCC-like tumors in anagen versus telogen hair follicles does not appear to be related to gross differences in *GLI2ΔN*

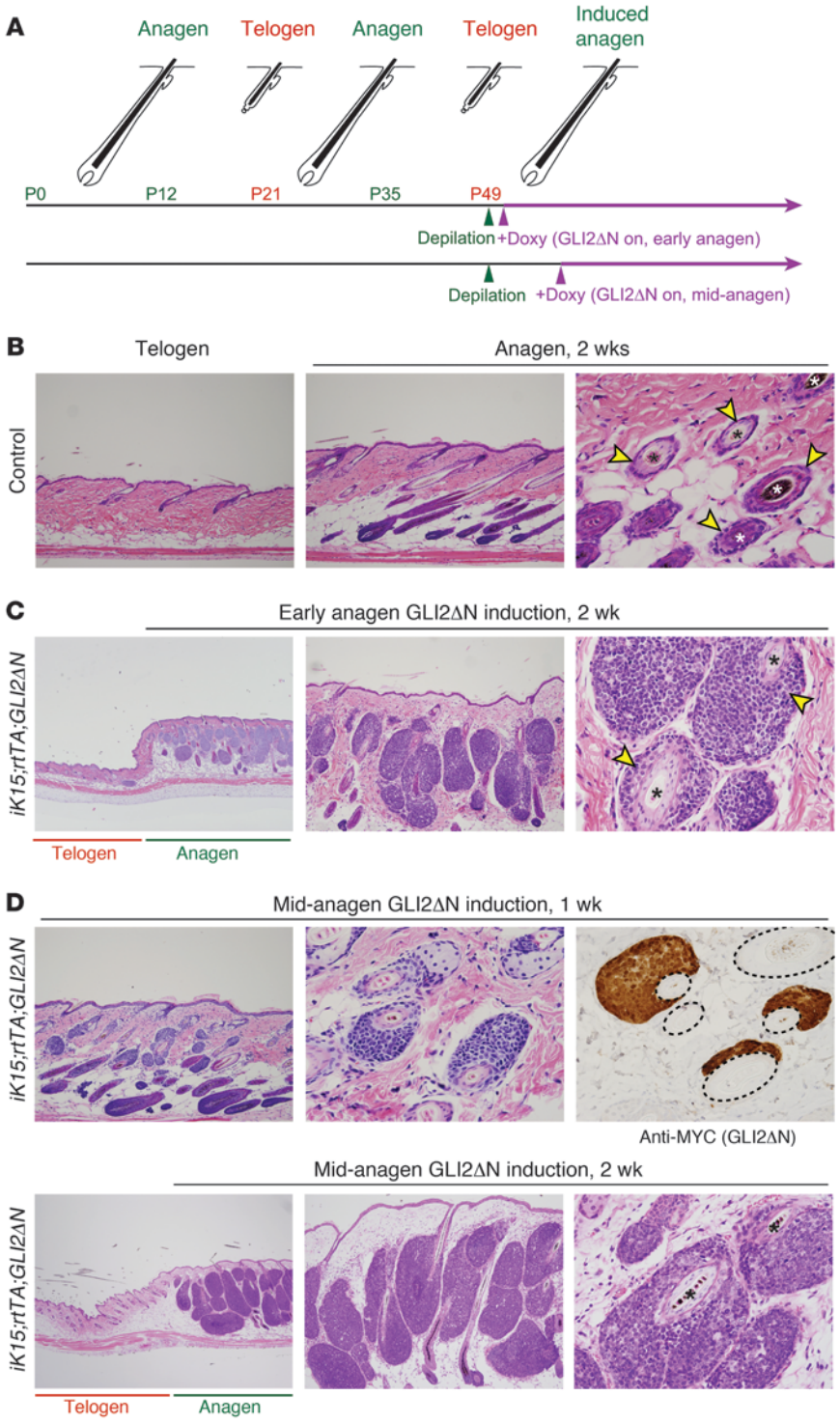

Figure 6
Anagen accelerates GLI2ΔN-driven tumorigenesis. (**A**) Hair growth cycle in dorsal skin showing timing of depilation (to induce anagen) and doxycycline treatment (to activate GLI2ΔN expression in either early or mid-anagen). (**B**) Depilation of control mice activates hair follicle growth, with anagen follicles extending into the subcutaneous adipose layer. Tangential section (right panel) shows outer root sheath compartment of the anagen follicle (arrowheads) and pigmented hair shafts (asterisks). Original magnification, ×100 (left and middle panels); ×400 (right panel). (**C**) Induction of GLI2ΔN in *iK15;rtTA;GLI2ΔN* mice during early anagen leads to widespread tumor development from growing hair follicles in 2 weeks, at a time when spontaneous tumors in adjacent skin are rare (left panel). In some areas, tumors are contiguous with and appear to replace the outer root sheath compartment of the anagen follicle (arrowheads in right panel). Original magnification, ×40 (left panel); ×100 (middle panel); ×400 (right panel). (**D**) GLI2ΔN induction for 1 week in mature hair follicles (mid-anagen) shows tumor derivation directly from the outer root sheath. Immunostaining for transgene (right panel) reveals GLI2ΔN expression in all regions exhibiting BCC-like changes. Dashed lines delineate hair follicles. Typical BCC-like tumors develop after an additional week of transgene expression (lower panels). Original magnification, ×100 (upper-left panel); ×400 (upper-middle and -right panels); ×40 (lower-left panel); ×100 (lower-middle panel); ×400 (lower-right panel).

transgene expression, protein accumulation, or transcriptional activity, based on in situ analysis of Hh/Gli target genes *Gli1* and *Ptch1* (Supplemental Figure 2). Together, these experiments provide evidence that BCC development occurs preferentially (but not exclusively) during the anagen phase of the hair cycle (29, 32) and are the first to our knowledge to directly test this concept using a conditional mouse model to activate oncogenic Hh signaling at different stages of the hair cycle.

BCC-like tumors can arise from the anagen follicle outer root sheath. Tumor cells frequently appeared contiguous with the follicle outer root sheath (Figure 6, B and C), raising the possibility that this transit-amplifying progenitor cell population (32) is a potential source of tumor progenitors in anagen. To address whether tumor nodules could arise directly from outer root sheath cells, we delayed transgene activation until 7 days after anagen induction (mid-anagen, Figure 6A) to allow for the proliferative expan-

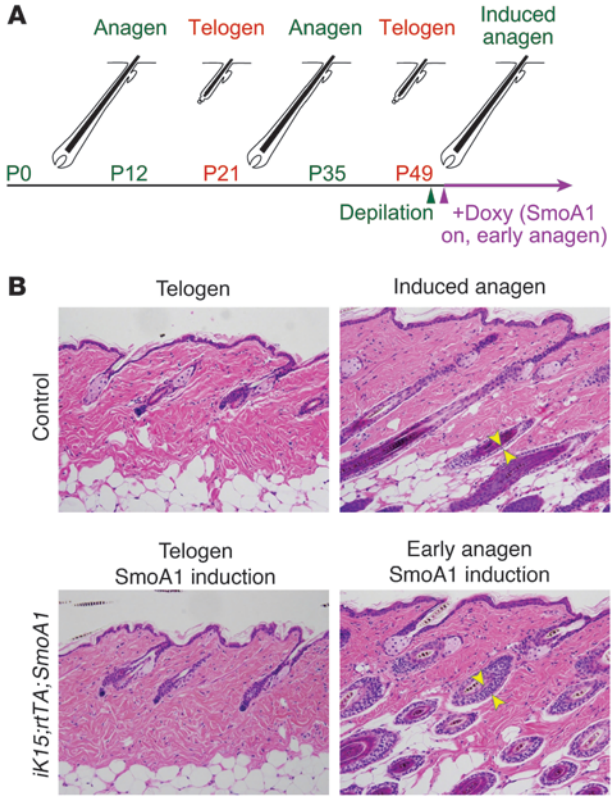

Figure 7
Oncogenic Smo drives outer root sheath hyperplasia but not nodular BCC-like tumor development. (**A**) Schematic depicting timing of depilation and transgene activation in *iK15;rtTA;SmoA1* mice. (**B**) In contrast to analogous GLI2ΔN-expressing mice, which produce nodular BCC-like tumors when the same experimental approach is used (Figure 6C), activation of SmoA1 in early anagen leads to hyperplasia of the outer root sheath (compare distance between arrowheads in upper- and lower-right panels) but no evidence of BCC-like tumors. Original magnification, ×200.

sion needed to assemble a mature anagen hair follicle (41). One week after transgene induction in mature anagen hair follicles, microscopic, GLI2ΔN-expressing tumor nodules were detected arising directly from the outer root sheath (Figure 6D), supporting the idea that this compartment contains cells capable of transformation by deregulated Hh/Gli signaling and may provide an expanded pool of potential tumor progenitors that accounts for the increased incidence of BCCs during anagen (29, 32). After an additional week of GLI2ΔN expression, large, nodular tumors had formed that filled much of the dermis in regions where anagen hair growth had been activated (Figure 6D).

Activated SMO is a weak oncogene in mouse skin that can be mimicked by low-level GLI2ΔN. Our findings using GLI2ΔN as the oncogenic driver establish that hair follicle stem cells in telogen are competent to form nodular skin tumors and that tumorigenesis is accelerated during anagen. We had previously shown that oncogenic human SMO (M2SMO) is a weak Hh pathway activator in skin and yielded basaloid follicular hamartomas rather than nodular BCCs or other BCC-like tumors, which are associated with high-level Hh signaling activity in both mice and humans (35, 36, 49). To further explore this issue in the context of stem cell targeting, we used *tetO-SmoA1* mice that we had previously generated (50) to produce *K15-CrePR1;R26-LSL-rtTA;tetO-SmoA1* (*iK15;rtTA;SmoA1*) triple-transgenic mice, and again performed transgene induction studies during early anagen (Figure 7A). In striking contrast to the nodular tumors seen in anagen-activated dorsal skin of *GLI2ΔN*-expressing mice (Figure 6C), mice expressing *SmoA1* exhibited modest outer root sheath hyperplasia (Figure 7B) but no evidence of frank tumor development. These findings indicate that SmoA1, using the same modeling strategy that yields robust tumors in response to GLI2ΔN, is not sufficient to drive BCC-like tumorigenesis from K15$^+$ follicle stem cells or their progeny.

We previously proposed that the absence of nodular BCC-like tumors in mice expressing activated SMO was due to relatively weak oncogenic signaling, based on the low expression level of Gli target genes in lesions resembling basaloid follicular hamartomas (arising in SMO mice) compared with BCCs (arising in Gli2 mice) (35). To directly test whether the level of Gli transcriptional activity is a determinant of tumor phenotype, we modified the doxycycline dosing regimen to induce different levels of GLI2ΔN in skin. Whereas GLI2ΔN-expressing mice treated with standard doses of doxycycline (GLI2ΔN-high) produced nodular and superficial BCC-like tumors, mice treated with low-dose doxycycline (GLI2ΔN-low) developed slow-growing basaloid tumors similar to those in mice expressing oncogenic SMO in skin (Figure 8A and refs. 35, 36). Although these lesions resemble human basaloid follicular hamartomas in several respects (49, 51, 52), as previously discussed (35), we favor a more conservative classification as basaloid hamartomas, with variable degrees of sebaceous hyperplasia.

Immunostaining for Ki67 revealed diffusely increased proliferation in BCC-like tumors in GLI2ΔN-high mice, with a low level of proliferation limited to the periphery of basaloid hamartomas in GLI2ΔN-low or SMO mice (Figure 8B), reflecting findings in human BCC and basaloid follicular hamartomas (49). MYC immunostaining to detect GLI2ΔN confirmed markedly reduced expression levels in hamartomatous proliferations arising in GLI2ΔN-low mice relative to uniformly robust expression in BCC-like tumors in GLI2ΔN-high mice (Figure 8C). These results support the concept that low-level oncogenic Hh/Gli signaling is an effective inducer of basaloid hamartomas, but not the nodular BCC-like skin tumors that are seen with higher-level signaling (25, 26, 31, 33, 35, 45).

Discussion

The cellular origin of BCC has been approached largely through descriptive studies using human tissue specimens and has been rather poorly understood. In the past, experimental studies rigorously addressing this have been hampered in part by the fact that BCCs rarely develop in wild-type mice, even after exposure to physical or chemical carcinogens that are potent inducers of BCC development in rats (reviewed in ref. 53). However, genetic models wherein different components of the Hh pathway are altered in cutaneous epithelia have yielded BCCs and related tumor types in mouse skin with high penetrance (reviewed in refs. 9, 10). Using multiple mouse models to control the timing and level of oncogenic Hh signaling activity and, most importantly, the particular cell populations where Hh signaling was altered, we have conclusively established that the transformation potential and varied BCC-like tumor phenotypes in skin are dictated by (a) the cell population

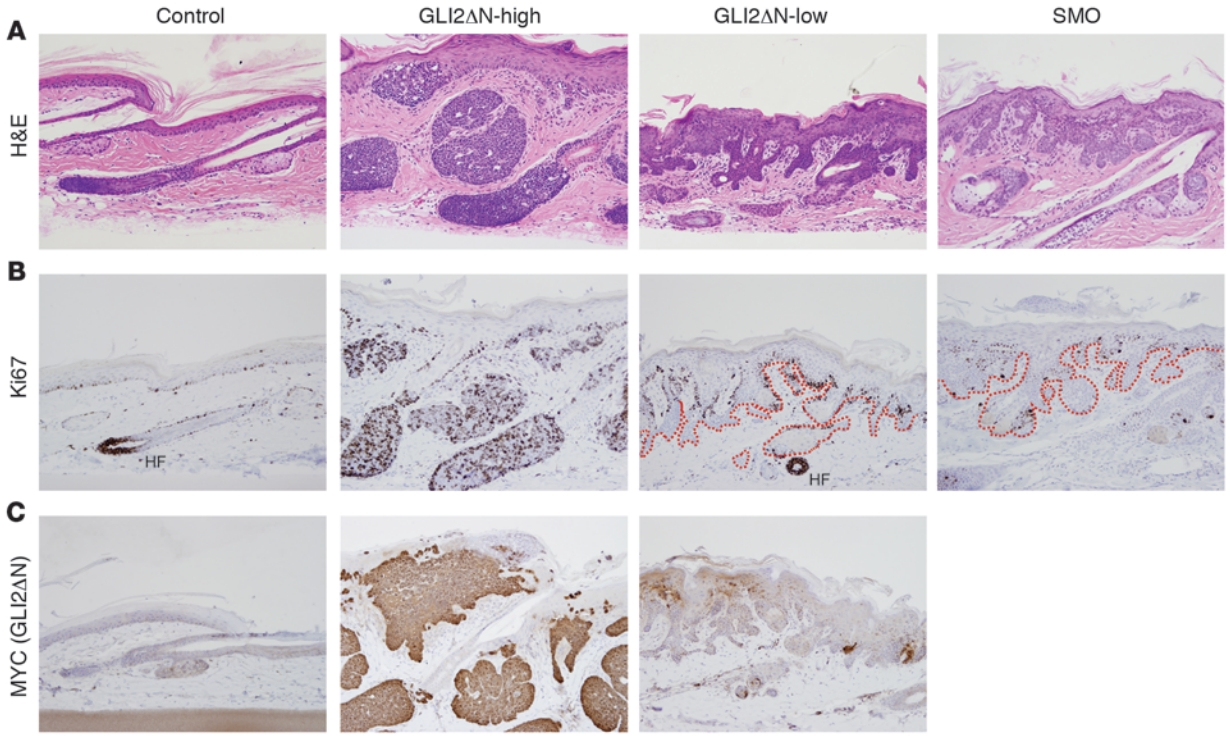

Figure 8
Low-level expression of GLI2ΔN gives rise to basaloid hamartomas instead of nodular BCC-like tumors. (**A**) Histology showing nodular BCC-like tumors in *iK5;rtTA;GLI2ΔN* mouse treated with 1 gm/kg doxycycline in chow and 200 μg/ml doxycycline in drinking water (GLI2ΔN-high), compared with basaloid hamartomas in *K5;rtTA;GLI2ΔN* mice treated with 2 μg/ml doxycycline (GLI2ΔN-low) in drinking water, which resemble lesions that arise in mice harboring a Cre-inducible *M2SMO* allele (SMO). (**B**) Ki67 reveals limited proliferation at the periphery of basaloid hamartomas arising in GLI2ΔN-low and SMO mice, compared with diffuse proliferation in nodular BCCs in GLI2ΔN-high mice. Dashed lines in right panels outline the extent of epithelial cells comprising hamartomas. HF indicates an anagen hair follicle matrix with robust Ki67 immunostaining. (**C**) MYC immunostaining to detect GLI2ΔN confirms low-level expression in GLI2ΔN-low mice. Original magnification, ×200 (**A**–**C**).

being targeted, (b) timing (relative to the hair cycle), and (c) level of oncogenic Hh signaling.

We find that multiple epithelial compartments in skin are competent to form BCC-like tumors in response to GLI2ΔN, but the particular tumor subtype differs based on the cells in which GLI2ΔN is active, indicating that while an oncogenic Hh signal is sufficient to drive tumorigenesis, tumor phenotype is strongly influenced by its cell of origin. Postnatal induction of GLI2ΔN in telogen follicle stem cells leads to the development of nodular BCC-like skin tumors (Figures 1 and 3), while induction in interfollicular epidermis or epidermis from hairless skin yields superficial BCC-like tumors (Figure 5); however, additional studies will be required to ascertain how closely these superficial tumors in mice mimic their human counterparts. An epidermal origin for superficial BCCs in humans is supported by histological studies examining microscopic tumors, which are first detected in interfollicular epidermis or the uppermost portion of the hair follicle, the infundibulum (54). Collectively, both human and mouse data argue that hair follicles are not required for the development of superficial BCCs, most of which appear to arise from interfollicular epidermis.

In contrast to superficial BCCs, several previous reports point to the follicle as a potential site of origin for nodular BCC in mouse (25–34) and rat (55), but the involvement of follicle stem cells in the development of these tumors was not addressed. Using *K15* and *Lgr5* promoter–driven Cre alleles, we show that progenitors of nodular, BCC-like tumors reside within the secondary hair germ and lower bulge stem cell compartments of the hair follicle (Figures 1, 3, and 5). Our data are in keeping with recently reported lineage-tracing studies in irradiated $Ptch^{+/-}$ mice that had developed basaloid skin tumors, nearly all of which appear to arise from K15-expressing cells (56). The presence of mixed BCC growth patterns in up to nearly 40% of human BCC samples (22) raises the possibility that nodular BCCs can expand upward to also involve epidermis as superficial BCCs, or vice versa, since hair follicle stem cell progeny migrate into the epidermis during wound healing (44, 57–59). Given the resistance of cells in much of the bulge to Hh-driven transformation (Figure 2 and ref. 24), it will be interesting to determine whether injury-induced mobilization and migration of these cells or their progeny into epidermis renders them competent to form tumors outside of the hair follicle stem cell niche.

In short-term induction studies using *K14-rtTA;tetO-GLI2ΔN* mice, we found that cells in the telogen bulge were resistant to GLI2ΔN-induced transformation. This appeared to be due to (a) impaired accumulation of GLI2ΔN in this cellular compartment, (b) a blunted proliferative response in bulge cells that do express detectable levels of GLI2ΔN, and (c) activation of apoptosis in bulge cells (Figure 4), which may eliminate potential tumor progenitors in this stem cell compartment. Induction of apoptosis has also been reported in neural stem cells engineered to express Gli1 (60), suggesting that this response may serve as a protective mechanism

against deregulated, high-level Hh/Gli signaling in other stem cell populations. Epithelial cells residing within the central isthmus, just above the follicle bulge, also appeared largely unaffected in these mice (Figure 4A). In this compartment, however, many cells did not contain detectable GLI2ΔN protein (Figure 4D), but additional studies will be required to assess whether this reflects focal deficiencies in transcription driven by the K14 and K5 promoters or modulation of Gli proteins at the post-translational level, which is likely to involve proteosome-mediated degradation (45–47).

The timing of GLI2ΔN transgene induction relative to the hair cycle has a profound effect on BCC-like tumor development. This is best studied in dorsal skin, where the kinetics of hair cycling is well defined (Figure 1D and ref. 41) and telogen follicles can be reliably induced to enter anagen by hair plucking or depilation. Although microscopic BCC-like tumors arose spontaneously from a subset of telogen hair follicles in dorsal skin by 2 weeks of GLI2ΔN expression, gross evidence of tumor development during the same time period was seen in skin containing anagen hair follicles (Figure 6). Accelerated tumorigenesis does not appear to be related to markedly greater accumulation of GLI2ΔN protein in anagen, as might have been expected (32, 45), since telogen-derived tumors and anagen-derived tumors had comparable levels of immunostaining for GLI2ΔN (Supplemental Figure 2). In addition, the transcriptional activity of GLI2ΔN also appears to be similar in telogen-initiated and anagen-initiated tumors, based on *Gli1* and *Ptch1* expression (Supplemental Figure 2).

Since anagen is characterized by robust proliferation of transit-amplifying stem cell progeny to reconstruct a mature follicle, accelerated tumorigenesis may reflect the ability of a small number of GLI2ΔN-expressing nascent tumor cells in telogen to rapidly expand into a detectable tumor mass under these growth-promoting conditions. This raises the possibility that in human BCC, quiescent follicle stem cells carrying mutations leading to Hh pathway activation may remain dormant until mobilized during early anagen or in response to another regenerative stimulus, when their selective growth advantage can lead to tumor formation. The rapid development of BCC-like nodules directly from the anagen outer root sheath (Figure 6D) is in keeping with this idea, and this finding identifies this transit-amplifying cell population as the likely cell of origin for BCCs that arise during anagen.

In addition to the important roles of cell of origin and hair cycling, we also show that GLI2ΔN expression levels define tumor phenotype, with low-level GLI2ΔN yielding basaloid hamartomas mimicking skin lesions in SMO-expressing mice (35, 36), rather than nodular BCC-like tumors (Figure 8). These data provide direct evidence supporting the hypothesis that a sufficiently high level of Hh signaling must be achieved to drive development of nodular BCC-like tumors (35). In addition, induction of oncogenic Smo in follicle stem cells, using the same strategy that yields multiple BCC-like tumors in response to GLI2ΔN, gives rise to a hyperplastic outer root sheath but no BCC-like tumors (Figure 7). These results are in general agreement with a recent study in which clonal, postnatal activation of a Cre-inducible Smo mutant failed to produce tumors from follicle stem cells or their progeny, but did lead to the development of basaloid skin tumors derived primarily from interfollicular epidermis (24). However, these lesions do not have the typical histological or gross appearance of nodular BCCs, which is in keeping with the idea that only high-level Hh signaling leads to BCC development (35). Establishing a definitive diagnosis in mouse models of cancer that is based on comparisons with human pathology can be challenging, particularly in skin, where there are major differences in tissue architecture between these two species. Nevertheless, the pattern of lineage markers, robust proliferation, and occasional areas of central necrosis seen in GLI2ΔN-expressing tumors described in this report are in keeping with the diagnosis of nodular, BCC-like tumors. Interestingly, the weak transforming potential of activated *Smo* alleles may be limited to skin, since *Smo* is a potent oncogene in cerebellum, where it gives rise to medulloblastomas with high penetrance when targeted to neuronal progenitors (50, 61, 62).

The results of our studies can be summarized as follows. (a) We have established the utility of a versatile new mouse model of cancer that can be readily adapted to study a variety of oncogenic pathways in different target organs. (b) We have shown that nodular BCC-like skin tumors in mice can arise from $Lgr5^+$ stem cells in the resting hair follicle and from basal cell compartments of the epidermis, growing hair follicle (outer root sheath), and sebaceous gland. These findings are in keeping with the varied histological presentations of human BCC, which include epidermis-associated superficial BCCs, nodular BCCs (which we propose are derived from hair follicles), and BCCs with sebaceous differentiation (22, 23, 63). (c) In contrast to other basal cell populations, stem cells within the bulge appear to be largely incapable of mounting a hyperplastic response to GLI2ΔN expression, although a fraction of these cells do activate expression of proliferation markers but appear destined to be eliminated via apoptosis. (d) We show that nodular BCC-like tumors do not form in mice expressing reduced levels of GLI2ΔN, but instead these mice develop basaloid hamartomas that are strikingly similar to lesions arising in mice expressing oncogenic Smo alleles. These findings provide direct evidence supporting the concept that full-blown nodular BCCs develop only in response to high-level Hh/Gli signaling activity, and may explain the reported lack of nodular tumors arising from follicle stem cells in Smo-expressing mice.

Methods

Mouse models

Generation and characterization of tetO-GLI2ΔN mice. The *tetO-GLI2ΔN* transgenic construct was generated as follows. A *Bam*HI-*Xba*I fragment, including MYC epitope–tagged human *GLI2* cDNA missing the amino-terminal repressor domain (*GLI2ΔN*), was excised from pCS2MT-GLI2 (39), which was provided by Erich Roessler and Maximilian Muenke (NIH, Bethesda, Maryland, USA). Cohesive ends were filled in for blunt-ended ligation into the *Eco*RV site of the pTet-Splice vector (Invitrogen), which contains a CMV promoter under the control of tet operon (*tetO*) sequences, SV40 intron and poly(A) signal, and modification to contain an additional *Not*I site. All cloning was verified by sequencing. A *Not*I-*Not*I fragment from *tetO-GLI2ΔN* was purified and injected into $(C57BL/6 \times SJL)F_2$ mouse eggs by members of the University of Michigan Transgenic Core; founders were identified by PCR using SV40 poly(A)–specific primers; and they were crossed with C57BL/6J breeders (The Jackson Laboratory) to establish transgenic lines. Progeny of 4 independent lines were crossed with *K5-tTA* mice (64) to screen for BCC-like tumor development in skin of bitransgenic *K5-tTA;tetO-GLI2ΔN* mice. Two lines with robust phenotypes, *tetO-GLI2ΔN*^{377} and *tetO-GLI2ΔN*^{380}, were used for the studies presented in this report, with the majority of experiments performed using the *tetO-GLI2ΔN*^{380} line. *tetO-GLI2ΔN* lines were crossed with C57BL/6 breeders for at least 6 generations.

Additional mouse strains. Several additional mouse lines carrying constitutive or hormone-inducible Cre alleles, or doxycycline-regulated tet trans-

activator alleles, were used in these studies (see Supplemental Figure 1 for partial listing and the predicted cell populations that are targeted). *K5-Cre* mice (65) were received from José Jorcano (CIEMAT, Madrid, Spain); *K5-CreERT2* mice (48), designated *K5-CreER* here, from Pierre Chambon and Daniel Metzger (Université de Strasbourg, Illkirch, France); *K15-CrePR1* mice (40) from George Cotsarelis (University of Pennsylvania, Philadelphia, Pennsylvania, USA); *Gt(ROSA)26Sor*$^{tm1(rtTA,EGFP)Nagy/J}$ mice (37), designated *R26-LSL-rtTA* here, from The Jackson Laboratory (stock number 005572); *Lgr5*$^{tm1(cre/ESR1)Cle}$ mice (66), designated *Lgr5-CreER* here, from The Jackson Laboratory (stock number 008875); *K5-rtTA* mice (64) from Adam Glick (Pennsylvania State University, State College, Pennsylvania, USA); and *Tg(KRT14-rtTA)F42Efu* mice (67), designated *K14-rtTA* here, from The Jackson Laboratory (stock number 008099). We previously described mice carrying a tet-inducible oncogenic *Smo* allele (*tetO-SmoA1*) (50) or Cre-inducible oncogenic human *SMO* allele (*K5-flxGFP-M2SMO*) (68).

Generating mice with inducible transgene expression. Precise spatial and temporal control of oncogenic Hh signaling was achieved in hair follicle stem cells and their progeny by adaption of a novel Cre-inducible and doxycycline-related mouse model (37) to control transgene expression. This model utilizes mice carrying 3 alleles: (a) a tissue-specific Cre driver, which may contain a hormone-inducible Cre allele (Supplemental Figure 1); (b) the Cre-inducible *R26-LSL-rtTA* strain (37); and (c) a *tetO-GLI2ΔN* or *tetO-SmoA1* effector strain (see Figure 1A and text for additional details). Details regarding hormone and doxycycline administration for transgene induction studies are described below. Mice were crossed according to standard protocols to generate triple-transgenic mice with the various genotypes described in the text. In addition, we generated *K14-rtTA;tetO-GLI2ΔN* and *K5-rtTA;tetO-GLI2ΔN* bitransgenic mice to achieve widespread expression of GLI2ΔN in basal cell layers of skin. All mice were housed and maintained according to University of Michigan institutional guidelines, and protocols for mouse experimentation were approved by the University of Michigan Committee on the Use and Care of Animals.

Genotyping. Genotyping was performed using the following primers and PCR parameters. For *K15-CrePR1*, *Lgr5-CreERT2*, *K5-Cre*, and *K5-CreER* mice, we amplified *Cre* using forward primer 5′-CATGCTTCATCGTCGGTCC-3′ and reverse primer 5′-GATCATCAGCTACACCAGAG-3′ (PCR parameters: 95°C for 5 minutes, [95°C for 30 seconds, 58°C for 30 seconds, 72°C for 30 seconds] for 35 cycles, 72°C for 5 minutes) to generate a 412-bp reaction product. For *K5-tTA* and *K5-rtTA* mice, we amplified *TA transactivator* using forward primer 5′-TTATTTGATCACCAAGGTGGAG-3′ and reverse primer 5′-CGATGGTAGACCCGTAATTGTT-3′ (PCR parameters: 95°C for 5 minutes [95°C for 30 seconds, 62°C for 40 seconds, 72°C for 40 seconds] for 35 cycles, 72°C for 2 minutes) to generate a 142-bp reaction product. For *R26-LSL-rtTA* mice, we either amplified *TA* (primers and PCR parameters as listed above) or *EGFP*, using forward primer 5′-GCACGACTTCTTCAAGTCCGCCATGCC-3′ and reverse primer 5′-GCGGATCTTGAAGTTCACCTTGATGCC-3′ (PCR parameters: 95°C for 4 minutes [95°C for 30 seconds, 72°C for 30 seconds, 72°C for 30 seconds] for 30 cycles, 72°C for 5 minutes) to generate a 280-bp reaction product. For *tetO-GLI2ΔN* and *tetO-SmoA1* mice, we amplified SV40 poly(A) using forward primer 5′-GGAACTGATGAATGGGAGCA-3′ and reverse primer 5′-GGGAGGTGTGGGAGGTTT-3′ (PCR parameters: 95°C for 5 minutes [94°C for 30 seconds, 57°C for 60 seconds, 72°C for 60 seconds] for 35 cycles, 72°C for 5 minutes) to generate a 522-bp reaction product. For *K14-rtTA* mouse genotyping, we used primer sequences provided by The Jackson Laboratory, with forward primer oIMR7862 (5′-CACGATACACCTGACTAGCTGGGTG-3′) and reverse primer oIMR7863 (5′-CATCACCCACAGGCTAGCGCCAACT-3′) (PCR parameters: 94°C for 3 minutes [94°C for 30 seconds, 67°C for 60 seconds, 72°C for 60 seconds] for 35 cycles, 72°C for 2 minutes) to generate an approximately 500-bp reaction product. For *R26R* mice, we amplified *lacZ* using forward primer 5′-GCTGGGATCCGCCATTGTCAGACATG-3′ and reverse primer oIMR7863 (5′-GCTGGAATTCCGCCGATACTGAC-3′) (PCR parameters: 95°C for 5 minutes [95°C for 30 seconds, 58°C for 40 seconds, 72°C for 40 seconds] for 35 cycles, 72°C for 2 minutes) to generate a 275-bp reaction product.

Transgene induction protocols

Transgene induction studies were performed during the prolonged resting phase of the hair cycle, which begins on day 49 (Figure 1D). Triple-transgenic mice carrying conditional *Cre* alleles were treated first with hormone to stimulate Cre recombinase activity/rtTA expression and then with doxycycline to induce *tetO*-regulated gene expression. Typically, for *iK15;rtTA;GLI2ΔN* mice, in which the bulge and secondary hair germ stem cell compartments are targeted (Supplemental Figure 1), dorsal hair was clipped and daily RU486 (Sigma-Aldrich) treatment was performed for 5 consecutive days ending on day 49. RU486 was applied topically in a cream formulation containing 2 mg RU486/g hand cream (Neutrogena Norwegian Formula Hand Cream, Fragrance-Free), which was prepared by incorporating 200 μl RU486 stock solution (20 mg RU486/ml absolute EtOH) into 2 g cream using a spatula. Each mouse received a daily dose of approximately 0.1 mg RU486 in cream. In some experiments, mice received two 5-day treatments of RU486 in cream, with the additional treatments starting on day 19. For experiments using *iLgr5;rtTA;GLI2ΔN* mice, Cre recombinase was activated using tamoxifen (Sigma-Aldrich) administered by oral gavage, with a daily dose of 0.1 mg tamoxifen/g body weight on 2 consecutive days starting on day 49. Tamoxifen stock was prepared at 20 mg/ml in corn oil. For focal activation of Cre function in the *iK5;rtTA;GLI2ΔN* model, a single low dose of tamoxifen (0.1 mg/mouse) was administered by oral gavage on day 48.

Doxycycline was used to activate expression of tet/doxycycline-responsive transgenes. For standard dosing, mice were fed chow containing 1 g doxycycline/kg chow (Bio-Serv), and for the first 3 days of treatment they also received 200 μg/ml doxycycline (Sigma-Aldrich) in drinking water with 5% sucrose. In experiments examining responses to reduced GLI2ΔN levels, mice were treated with low-dose doxycycline, at either 2 μg/ml or 0.4 μg/ml doxycycline in water with 5% sucrose. Based on an approximate daily food intake of 4 g/mouse and water intake of 6 ml/mouse (69), mice receiving standard dosing with doxycycline chow consumed approximately 4 mg doxycycline/d, whereas mice with reduced dosing in water consumed between 12 and 2.4 μg doxycycline/d.

In some experiments, GLI2ΔN transgene was induced in mice either shortly after activation of dorsal hair growth (early anagen) or in mature, growing hair follicles (mid-anagen). Mice were treated with RU486 or tamoxifen, and hair growth was induced by Nair or hair plucking at approximately 7 weeks of age. For early anagen experiments, standard dosing with doxycycline was initiated 1 day later. For mid-anagen experiments, doxycycline was started 7 days later to allow for hair follicle maturation.

Tissue collection, immunostaining, and in situ hybridization

Tissue samples were fixed in neutral-buffered formalin at room temperature or in 4% paraformaldehyde at 4°C overnight, transferred to 70% ethanol, processed, and embedded in paraffin. For frozen sections, tissue was fixed in 4% paraformaldehyde at 4°C for 1 hour, transferred to 30% sucrose/PBS overnight, embedded in Tissue-Tek O.C.T. Compound (Sakura), and frozen.

For immunostaining, sections were deparaffinized, and antigen retrieval was performed using boiling citrate-based buffer or Trilogy reagent (Cell Marque). Sections were treated in 3% H_2O_2 for 7 minutes, blocked in 2% normal goat serum in PBS for 30 minutes, and incubated at 4°C overnight with primary antibody. The following antibodies and dilutions were used:

anti-keratins K1, K5, and K6 (Covance) 1:1,000; anti–keratin K15 (Thermo Scientific) 1:500; anti–keratin K17 (provided by Pierre Coulombe, Johns Hopkins University, Baltimore, Maryland, USA) 1:4,000; anti-Ki67 (clone SP6, Thermo Scientific) 1:200; anti-Sox9 (Millipore) 1:1,000; PCNA (Thermo Scientific) 1:300; and anti–cleaved caspase-3 (Cell Signaling Technology) 1:200. For immunohistochemistry studies, primary antibodies were detected using the VECTASTAIN Peroxidase ABC Standard kit (Vector Laboratories, PK-4001), and visualization was performed using DAB as chromogen with a hematoxylin counterstain. To detect the MYC-tagged GLI2ΔN transgene product, sections were blocked for 1 hour with blocking reagent (M.O.M. kit, Vector Laboratories, PK-2200) and incubated at 4°C overnight with Myc-Tag (9B11) mouse monoclonal antibody (Cell Signaling Technology), diluted 1:2,000 in PBS. The remainder of the immunostaining protocol was performed following the manufacturer's instructions with minor modifications.

For double immunofluorescence staining, secondary antibodies conjugated with DyLight 488 or DyLight 549 (Jackson ImmunoResearch Laboratories Inc.) were used at a 1:400 dilution. For immunofluorescence visualization, sections were mounted with ProLong Gold Antifade Reagent with DAPI (Invitrogen). Cell counts were performed to enumerate $Ki67^+$ proliferating cells in bulge compartments after 2 and 5 days of GLI2ΔN expression and to assess the proportion of MYC^+ cells that were also $Ki67^+$ in bulge, epidermis, and sebaceous gland.

In situ hybridization was performed on paraffin-embedded sections of neutral buffered formalin–fixed tissue. Riboprobe sequences, probe preparation, and hybridization protocols have been described elsewhere (35).

Statistics

Statistical analysis was performed using 1-way ANOVA with Bonferroni post-hoc multiple comparisons. Data are presented as mean ± SEM, with *P* values less than 0.05 considered significant. Data were analyzed using PASW Statistics 18 software (SPSS Inc.).

Note added in proof. After submission of a revised version of this manuscript, two reports were published showing the development of Hh pathway driven skin tumors derived from hair follicle stem cells following wounding-induced migration into interfollicular epidermis (70, 71).

Acknowledgments

We thank Ben Allen, Eric Fearon, Deborah Gumucio, Marina Pasca di Magliano, and members of the Dlugosz laboratory for comments on the manuscript. We are grateful to Pierre Coulombe, Daniel Metzger, Pierre Chambon, José Jorcano, Erich Roessler, and Maximilian Muenke for providing mice and/or reagents. We gratefully acknowledge Galina Gavrilina and the Transgenic Animal Model Core of the University of Michigan's Biomedical Research Core Facilities for production of *tetO-GLI2ΔN* transgenic mice. The work in this report was supported by NIH grants CA087837 and AR045973 and a gift from the Helen L. Kay Charitable Trust. Core support was provided by the University of Michigan Comprehensive Cancer Center (CA46592).

Received for publication January 6, 2011, and accepted in revised form March 2, 2011.

Address correspondence to: Andrzej A. Dlugosz, University of Michigan Medical School, Rm 3316 Cancer Center, SPC 5932, 1500 East Medical Center Drive, Ann Arbor, Michigan 48109-0932, USA. Phone: 734.647.9482; Fax: 734.763.4575; E-mail: dlugosza@umich.edu.

1. Visvader JE. Cells of origin in cancer. *Nature*. 2011; 469(7330):314–322.
2. Owens DM, Watt FM. Contribution of stem cells and differentiated cells to epidermal tumours. *Nat Rev Cancer*. 2003;3(6):444–451.
3. Perez-Losada J, Balmain A. Stem-cell hierarchy in skin cancer. *Nat Rev Cancer*. 2003;3(6):434–443.
4. Stenn KS, Paus R. Controls of hair follicle cycling. *Physiol Rev*. 2001;81(1):449–494.
5. Blanpain C, Fuchs E. Epidermal stem cells of the skin. *Annu Rev Cell Dev Biol*. 2006;22:339–373.
6. Epstein EH. Basal cell carcinomas: attack of the hedgehog. *Nat Rev Cancer*. 2008;8(10):743–754.
7. Barakat MT, Humke EW, Scott MP. Learning from Jekyll to control Hyde: Hedgehog signaling in development and cancer. *Trends Mol Med*. 2010; 16(8):337–348.
8. McMahon AP, Ingham PW, Tabin CJ. Developmental roles and clinical significance of hedgehog signaling. *Curr Top Dev Biol*. 2003;53:1–114.
9. Teglund S, Toftgard R. Hedgehog beyond medulloblastoma and basal cell carcinoma. *Biochim Biophys Acta*. 2010;1805(2):181–208.
10. Saran A. Basal cell carcinoma and the carcinogenic role of aberrant Hedgehog signaling. *Future Oncol*. 2010;6(6):1003–1014.
11. St-Jacques B, et al. Sonic hedgehog signaling is essential for hair development. *Curr Biol*. 1998; 8(19):1058–1068.
12. Chiang C, et al. Essential role for sonic hedgehog during hair follicle morphogenesis. *Dev Biol*. 1999; 205(1):1–9.
13. Gritli-Linde A, et al. Abnormal hair development and apparent follicular transformation to mammary gland in the absence of hedgehog signaling. *Dev Cell*. 2007;12(1):99–112.
14. Bai CB, Auerbach W, Lee JS, Stephen D, Joyner AL. Gli2, but not Gli1, is required for initial Shh signaling and ectopic activation of the Shh pathway. *Development*. 2002;129(20):4753–4761.
15. Mill P, et al. Sonic hedgehog-dependent activation of Gli2 is essential for embryonic hair follicle development. *Genes Dev*. 2003;17(2):282–294.
16. Wang LC, et al. Regular articles: conditional disruption of hedgehog signaling pathway defines its critical role in hair development and regeneration. *J Invest Dermatol*. 2000;114(5):901–908.
17. Kurzen H, Esposito L, Langbein L, Hartschuh W. Cytokeratins as markers of follicular differentiation: an immunohistochemical study of trichoblastoma and basal cell carcinoma. *Am J Dermatopathol*. 2001; 23(6):501–509.
18. Jih DM, Lyle S, Elenitsas R, Elder DE, Cotsarelis G. Cytokeratin 15 expression in trichoepitheliomas and a subset of basal cell carcinomas suggests they originate from hair follicle stem cells. *J Cutan Pathol*. 1999; 26(3):113–118.
19. Kruger K, Blume-Peytavi U, Orfanos CE. Basal cell carcinoma possibly originates from the outer root sheath and/or the bulge region of the vellus hair follicle. *Arch Dermatol Res*. 1999;291(5):253–259.
20. Rapini RP. Follicular differentiation in basal cell carcinoma and the trend to designate benign or questionable lesions as malignant. *J Am Acad Dermatol*. 2002;47(5):792–794.
21. Donovan J. Review of the hair follicle origin hypothesis for basal cell carcinoma. *Dermatol Surg*. 2009; 35(9):1311–1323.
22. Sexton M, Jones DB, Maloney ME. Histologic pattern analysis of basal cell carcinoma. Study of a series of 1039 consecutive neoplasms. *J Am Acad Dermatol*. 1990;23(6 pt 1):1118–1126.
23. Crowson AN. Basal cell carcinoma: biology, morphology and clinical implications. *Mod Pathol*. 2006; 19(suppl 2):S127–S147.
24. Youssef KK, et al. Identification of the cell lineage at the origin of basal cell carcinoma. *Nat Cell Biol*. 2010;12(3):299–305.
25. Grachtchouk M, et al. Basal cell carcinomas in mice overexpressing Gli2 in skin. *Nat Genet*. 2000; 24(3):216–217.
26. Nilsson M, et al. Induction of basal cell carcinomas and trichoepitheliomas in mice overexpressing GLI-1. *Proc Natl Acad Sci U S A*. 2000;97(7):3438–3443.
27. Aszterbaum M, et al. Ultraviolet and ionizing radiation enhance the growth of BCCs and trichoblastomas in patched heterozygous knockout mice. *Nat Med*. 1999;5(11):1285–1291.
28. Adolphe C, Hetherington R, Ellis T, Wainwright B. Patched1 functions as a gatekeeper by promoting cell cycle progression. *Cancer Res*. 2006;66(4):2081–2088.
29. Mancuso M, et al. Hair cycle-dependent basal cell carcinoma tumorigenesis in Ptc1neo67/+ mice exposed to radiation. *Cancer Res*. 2006;66(13):6606–6614.
30. Mancuso M, et al. Basal cell carcinoma and its development: insights from radiation-induced tumors in Ptch1-deficient mice. *Cancer Res*. 2004;64(3):934–941.
31. Svard J, et al. Genetic elimination of Suppressor of fused reveals an essential repressor function in the mammalian Hedgehog signaling pathway. *Dev Cell*. 2006;10(2):187–197.
32. Oro AE, Higgins K. Hair cycle regulation of Hedgehog signal reception. *Dev Biol*. 2003;255(2):238–248.
33. Hutchin ME, et al. Sustained Hedgehog signaling is required for basal cell carcinoma proliferation and survival: conditional skin tumorigenesis recapitulates the hair growth cycle. *Genes Dev*. 2005; 19(2):214–223.
34. Villani RM, Adolphe C, Palmer J, Waters MJ, Wainwright BJ. Patched1 inhibits epidermal progenitor cell expansion and basal cell carcinoma formation by limiting Igfbp2 activity. *Cancer Prev Res (Phila)*. 2010; 3(10):1222–1234.
35. Grachtchouk V, et al. The magnitude of hedgehog

signaling activity defines skin tumor phenotype. *EMBO J*. 2003;22(11):2741–2751.
36. Yang SH, et al. Pathological responses to oncogenic Hedgehog signaling in skin are dependent on canonical Wnt/beta-catenin signaling. *Nat Genet*. 2008;40(9):1130–1135.
37. Belteki G, et al. Conditional and inducible transgene expression in mice through the combinatorial use of Cre-mediated recombination and tetracycline induction. *Nucleic Acids Res*. 2005;33(5):e51.
38. Sheng H, et al. Dissecting the oncogenic potential of Gli2: deletion of an NH(2)-terminal fragment alters skin tumor phenotype. *Cancer Res*. 2002; 62(18):5308–5316.
39. Roessler E, et al. A previously unidentified amino-terminal domain regulates transcriptional activity of wild-type and disease-associated human GLI2. *Hum Mol Genet*. 2005;14(15):2181–2188.
40. Morris RJ, et al. Capturing and profiling adult hair follicle stem cells. *Nat Biotechnol*. 2004;22(4):411–417.
41. Muller-Rover S, et al. A comprehensive guide for the accurate classification of murine hair follicles in distinct hair cycle stages. *J Invest Dermatol*. 2001; 117(1):3–15.
42. Vidal VP, Ortonne N, Schedl A. SOX9 expression is a general marker of basal cell carcinoma and adnexal-related neoplasms. *J Cutan Pathol*. 2008; 35(4):373–379.
43. Jaks V, et al. Lgr5 marks cycling, yet long-lived, hair follicle stem cells. *Nat Genet*. 2008;40(11):1291–1299.
44. Snippert HJ, et al. Lgr6 marks stem cells in the hair follicle that generate all cell lineages of the skin. *Science*. 2010;327(5971):1385–1389.
45. Huntzicker EG, Estay IS, Zhen H, Lokteva LA, Jackson PK, Oro AE. Dual degradation signals control Gli protein stability and tumor formation. *Genes Dev*. 2006;20(3):276–281.
46. Pan Y, Bai CB, Joyner AL, Wang B. Sonic hedgehog signaling regulates Gli2 transcriptional activity by suppressing its processing and degradation. *Mol Cell Biol*. 2006;26(9):3365–3377.
47. Bhatia N, et al. Gli2 is targeted for ubiquitination and degradation by beta-TrCP ubiquitin ligase. *J Biol Chem*. 2006;281(28):19320–19326.
48. Indra AK, et al. Temporally-controlled site-specific mutagenesis in the basal layer of the epidermis: comparison of the recombinase activity of the tamoxifen-inducible Cre-ER(T) and Cre-ER(T2) recombinases. *Nucleic Acids Res*. 1999;27(22):4324–4327.
49. Jih DM, et al. Familial basaloid follicular hamartoma: lesional characterization and review of the literature. *Am J Dermatopathol*. 2003;25(2):130–137.
50. Michael LE, et al. Bmi1 is required for Hedgehog pathway-driven medulloblastoma expansion. *Neoplasia*. 2008;10(12):1343–1349.
51. Mills O, Thomas LB. Basaloid follicular hamartoma. *Arch Pathol Lab Med*. 2010;134(8):1215–1219.
52. Saxena A, Shapiro M, Kasper DA, Fitzpatrick JE, Mellette JR Jr. Basaloid follicular hamartoma: a cautionary tale and review of the literature. *Dermatol Surg*. 2007;33(9):1130–1135.
53. Dlugosz A, Merlino G, Yuspa SH. Progress in Cutaneous Cancer Research. *J Investig Dermatol Symp Proc*. 2002;7(1):17–26.
54. Zackheim HS. Origin of the human basal cell epithelioma. *J Invest Dermatol*. 1963;40:283–297.
55. Zackheim HS. Experimental basal cell carcinoma in the rat. In: Maibach H, Lowe N, eds. *Models in Dermatology*. Basel, Switzerland: Karger Publishers; 1985:89–97.
56. Wang GY, Wang J, Mancianti ML, Epstein EH Jr. Basal cell carcinomas arise from hair follicle stem cells in ptch1(+/–) mice. *Cancer Cell*. 2011;19(1):114–124.
57. Ito M, et al. Stem cells in the hair follicle bulge contribute to wound repair but not to homeostasis of the epidermis. *Nat Med*. 2005;11(12):1351–1354.
58. Ito M, et al. Wnt-dependent de novo hair follicle regeneration in adult mouse skin after wounding. *Nature*. 2007;447(7142):316–320.
59. Jensen KB, et al. Lrig1 expression defines a distinct multipotent stem cell population in mammalian epidermis. *Cell Stem Cell*. 2009;4(5):427–439.
60. Galvin KE, Ye H, Erstad DJ, Feddersen R, Wetmore C. Gli1 induces G2/M arrest and apoptosis in hippocampal but not tumor-derived neural stem cells. *Stem Cells*. 2008;26(4):1027–1036.
61. Hallahan AR, et al. The SmoA1 mouse model reveals that notch signaling is critical for the growth and survival of sonic hedgehog-induced medulloblastomas. *Cancer Res*. 2004;64(21):7794–7800.
62. Hatton BA, et al. The Smo/Smo model: hedgehog-induced medulloblastoma with 90% incidence and leptomeningeal spread. *Cancer Res*. 2008; 68(6):1768–1776.
63. Steffen CH, Ackerman AB. Basal cell carcinoma with sebaceous differentiation. In: Steffen CH, Ackerman AB, eds. *Neoplasms with Sebaceous Differentiation*. Philadelphia, Pennsylvania, USA: Lea and Febiger; 1994:577–596.
64. Diamond I, Owolabi T, Marco M, Lam C, Glick A. Conditional gene expression in the epidermis of transgenic mice using the tetracycline-regulated transactivators tTA and rTA linked to the keratin 5 promoter. *J Invest Dermatol*. 2000;115(5):788–794.
65. Ramirez A, et al. A keratin K5Cre transgenic line appropriate for tissue-specific or generalized Cre-mediated recombination. *Genesis*. 2004;39(1):52–57.
66. Barker N, et al. Identification of stem cells in small intestine and colon by marker gene Lgr5. *Nature*. 2007;449(7165):1003–1007.
67. Nguyen H, Rendl M, Fuchs E. Tcf3 governs stem cell features and represses cell fate determination in skin. *Cell*. 2006;127(1):171–183.
68. Allen M, et al. Hedgehog signaling regulates sebaceous gland development. *Am J Pathol*. 2003; 163(6):2173–2178.
69. Bachmanov AA, Reed DR, Beauchamp GK, Tordoff MG. Food intake, water intake, and drinking spout side preference of 28 mouse strains. *Behav Genet*. 2002;32(6):435–443.
70. Wong SY, Reiter JF. From the Cover: Wounding mobilizes hair follicle stem cells to form tumors. *Proc Natl Acad Sci U S A*. 2011;108(10):4093–4098.
71. Kasper M, et al. Wounding enhances epidermal tumorigenesis by recruiting hair follicle keratinocytes. *Proc Natl Acad Sci U S A*. 2011;108(10):4099–4104.